A&A 383, 1–13 (2002)
DOI: 10.1051/0004-6361:20011482
© ESO 2002

Astronomy & Astrophysics

Nuclear and global X-ray properties of LINER galaxies: *Chandra* and *BeppoSAX* results for Sombrero and NGC 4736

S. Pellegrini[1], G. Fabbiano[2], F. Fiore[3], G. Trinchieri[4], and A. Antonelli[3]

[1] Università di Bologna, Dipartimento di Astronomia, via Ranzani 1, 40127 Bologna, Italy
[2] Harvard-Smithsonian Center for Astrophysics, 60 Garden Street, Cambridge, MA 02138, USA
e-mail: pepi@head-cfa.harvard.edu
[3] Osservatorio Astronomico di Roma, via Frascati 33, 00044 Monteporzio Catone, Italy
e-mail: fiore@quasar.mporzio.astro.it; angelo@coma.mporzio.astro.it
[4] Osservatorio Astronomico di Brera, via Brera 28, 20121 Milan, Italy
e-mail: ginevra@brera.mi.astro.it

Received 23 July 2001 / Accepted 22 October 2001

Abstract. We report on the 0.1–100 keV *BeppoSAX* observations of two nearby LINER galaxies, Sombrero and NGC 4736. *Chandra* ACIS-S observations supplement this broad-beam spectral study with a high resolution look into the nuclear region, and show a dominating central point source in Sombrero and a complex X-ray binary dominated/starburst region in NGC 4736. A compact non-thermal radio source, present in the nucleus of both galaxies, coincides with the central source in Sombrero, while in NGC 4736 its X-ray counterpart is a much fainter point source, not the brightest of the central region. On the basis of these and other results, we conclude that the LINER activity is linked to the presence of a low luminosity AGN in Sombrero and to a recent starburst in NGC 4736, and that *Chandra*'s spectroscopic capabilities coupled to high resolution imaging are essential to establish the origin of the nuclear activity.

Key words. galaxies: spiral – galaxies: individual: NGC 4594, NGC 4736 – galaxies: active – galaxies: nuclei – X-rays: galaxies

1. Introduction

Optical spectroscopic surveys showed that low ionization nuclear emission line regions (LINERs, Heckman 1980) are very common among ellipticals and early type spirals (Ho et al. 1997). It is also currently believed that most galactic spheroids host supermassive black holes, based on *Hubble Space Telescope* (*HST*) stellar or ionized gas spectroscopy coupled to dynamical modeling (e.g., Richstone et al. 1998). So, it has become natural to ask whether AGN activity stops at Seyfert galaxies or extends down to lower luminosities, including LINERs. The answer to this question has important consequences for the history of accretion in the Universe (e.g., Haiman & Menou 2000). The LINER emission, though, need not be powered by AGN-like activity: collisional ionization by shocks and/or photoionization by the UV radiation from hot, young stars were also suggested as possible mechanisms (Terlevich et al. 1992; Alonso-Herrero et al. 2000). Observational support for this interpretation, in some cases, comes from optical and ultraviolet *HST* observations (e.g., Maoz et al. 1995) and from infrared studies (Larkin et al. 1998).

An important way of discriminating between different emission mechanisms is to observe LINERs in hard X-rays, where the AGN presence is easily identifiable, even when it is obscured by intervening matter (e.g., the LINER NGC 6240 turned out to be an obscured, high luminosity AGN from hard X-ray observations; Vignati et al. 1999). For this reason we observed Sombrero (NGC 4594) and NGC 4736 with *BeppoSAX* over 0.1–100 keV, as they are early type spirals hosting two of the closest examples of LINER activity (Table 1). Thanks to their proximity, they are excellent targets to explore the questions raised above and have been subject to thorough studies at various wavelengths, including high angular resolution observations with *HST*, the *ROSAT* HRI and the VLA.

However, a *BeppoSAX* study is severely limited by the available angular resolution, as are all the reports so far on the hard X-ray properties of LINERs based on spectra from a few arcminute beams. These show power laws

Send offprint requests to: S. Pellegrini,
e-mail: pellegrini@bo.astro.it

Article published by EDP Sciences and available at http://www.aanda.org or http://dx.doi.org/10.1051/0004-6361:20011482

that could equally come from an active nucleus or the collective emission of X-ray binaries [see the reviews by Fabbiano (1996) and Serlemitsos et al. (1996); and Ptak et al. (1999)]. When the analysis of the *BeppoSAX* data was complete, the *Chandra* observations of our target galaxies became available in the public archive, providing us with the unique opportunity to supplement our study with a very high resolution look into the nuclear regions. We therefore added the analysis of these data to our work. The *Chandra* observation of Sombrero was reported as part of a snapshot survey of faint nearby AGNs (Ho et al. 2001); we considered more in detail those data here. After submission of this paper, a preprint appeared on the astro-ph archive discussing in detail the overall *Chandra* observation of NGC 4736 (Eracleous et al. 2001); our analysis is limited to the centermost region only.

1.1. Properties of the target galaxies

At the nucleus of Sombrero, identified as a LINER (Heckman 1980), high resolution *HST* spectroscopy confirmed the presence of a central dark object of 10^9 $M_\odot$ and also revealed a faint broad $H\alpha$ component with full width at zero intensity of $\approx$5200 km s^{-1} (Kormendy et al. 1996). This nucleus hosts a compact and variable radio continuum source (Thean et al. 2000) and is a pointlike source in an *HST* image at 3400 Å (Crane et al. 1993).

In the X-ray, a *ROSAT* HRI image showed a pointlike central source, clumpy emission associated with the disk and diffuse or not resolved emission from the bulge (Fabbiano & Juda 1997, hereafter FJ). How much of this diffuse emission comes from a hot medium and how much from the integrated emission of evolved stellar sources could not be established. *ROSAT* PSPC spectra of the central circles of $1'$ and $2'$ radius indicate a steeper photon index (from $\Gamma = 1.76^{+0.44}_{-0.36}$ to $\Gamma = 1.84^{+0.41}_{-0.29}$) for the larger aperture, which FJ interpreted as an indication that the extended HRI emission is relatively soft. Nicholson et al. (1998) obtain $\Gamma = 1.63 \pm 0.05$ and a column density $N_{\rm H} = 5.3 \times 10^{20}$ cm^{-2} from the combined *ASCA* and *ROSAT* spectra; allowing for contamination by soft emission, the column density to the power law is 2.9×10^{21} cm^{-2}. Ptak et al. (1999), from combined *ASCA* and *ROSAT* data, find thermal emission with very low abundance (<0.1 $Z_\odot$) coupled to a power law of $\Gamma = 1.97^{+0.33}_{-0.29}$ absorbed by an excess $N_{\rm H} < 1.7 \times 10^{22}$ cm^{-2} over the Galactic value. Recently, Ho et al. (2001) report the first results from an arcsecond resolution snapshot survey of nearby galaxies performed by *Chandra*. In their morphological classification into four classes of the X-ray images obtained, Sombrero belongs to the class of objects with a "dominant nuclear source".

NGC 4736, a LINER2 galaxy (Ho et al. 1997), shows various pieces of evidence suggesting star formation that took place in its recent past. Balmer absorption lines and strong CO absorption indicate a nuclear starburst that occurred $\sim$1 Gyr ago (Wong & Blitz 2000). A bright optical ring is prominent in HI (Mulder & van Driel 1993), molecular gas (Gerin et al. 1991) and Hα (Pogge 1989). A younger stellar population is also revealed by 6cm radio continuum observations of compact HII regions associated with hot, young stars and young supernova remnants (Turner & Ho 1994) and by near-infrared spectra (Larkin et al. 1998). The nuclear region hosts a compact non-thermal radio continuum source (Turner & Ho 1994) and a bright UV point source revealed by *HST* (Maoz et al. 1995).

A *ROSAT* PSPC pointing showed within the central few kpc a compact source plus an extended distribution of hot gas ($kT \sim 0.3$ keV) contributing 30–35% of the total observed 0.1–2 keV flux (Cui et al. 1997). *ROSAT* HRI data showed 12 discrete sources superimposed on the optical disk and ring regions, likely X-ray binaries (hereafter XRBs), supernova remnants or recent supernovae; the brightest source was by far the galactic "nucleus" (Roberts et al. 1999, hereafter R99). The combined PSPC and *ASCA* spectrum (R99) is composed of a hard continuum, equally well modeled with a power law (with $\Gamma \sim 1.7$) or bremsstrahlung emission (with $kT \sim 8$ keV). The soft thermal emission was modeled with a two-temperature plasma (of $kT = 0.1$ and 0.6 keV) and solar abundance. A Fe Kα line may also be present at $6.81^{+0.13}_{-0.28}$ keV.

2. Spatial analysis

2.1. BeppoSAX observations

Sombrero and NGC 4736 were observed with the Low Energy Concentrator Spectrometer (LECS, Parmar et al. 1997), the Medium Energy Concentrator Spectrometer (MECS, Boella et al. 1997) and the Phoswich Detector system (PDS). The latter is a collimated instrument, operating in rocking mode, that covers the 13–300 keV energy band. It has a triangular response with FWHM of $\sim$1°.3 (Frontera et al. 1997). Its data were reduced using the variable risetime threshold technique to reject particle background (Fiore et al. 1999). The journal of these observations is given in Table 2.

BeppoSAX was pointed to the optical centers of the galaxies, on which the X-ray emission is peaked (Fig. 1) within the accuracy with which positions are given by the satellite (Boella et al. 1997). In the MECS image of Sombrero there is a prominent source at RA = 12 39 45.2, Dec = −11 38 49.6; we identify it with a bright 9.7 mag G0 star (HD 110086). The absence of this source in the harder 4.5–10 keV image indicates its soft nature and supports its identification. We determined the spatial extent of the galactic emission using the MECS data[1] from azimuthally averaged brightness profiles in concentric annuli centered on the X-ray centroids. The background profile in the same detector region was estimated from event

[1] The PSF of the MECS includes 80% of photons of energies $\geq$1.5 keV within a radius of 2′.7 (Boella et al. 1997). The LECS PSF is broader than this below 1 keV and similar above 2 keV.

Table 1. General galaxy properties.

Galaxy	Type[a]	RA[a] (J2000)	Dec[a] (J2000)	d [b] (Mpc)	$B_{\rm T}^0$ [a] (mag)	$\log L_{\rm B}$ [c] ($L_\odot$)	$N_{\rm H,Gal}$ [d] ($\rm cm^{-2}$)
Sombrero	Sa	$12^{\rm h}39^{\rm m}59\overset{\rm s}{.}4$	$-11^\circ37'23''$	9.4	8.38	10.79	3.5×10^{20}
NGC 4736	Sab	$12^{\rm h}50\overset{\rm m}{.}53\overset{\rm s}{.}6$	$+41^\circ07'10''$	5.9	8.75	10.23	1.4×10^{20}

[a] From de Vaucouleurs et al. (1991). $B_{\rm T}^0$ is the total B magnitude, corrected for extinction.
[b] Distance from Ajhar et al. (1997) for Sombrero et al. (1994) for NGC 4736.
[c] Total B-band luminosity, derived using the indicated distance and $B_{\rm T}^0$.
[d] Galactic neutral hydrogen column density from Stark et al. (1992).

Table 2. *BeppoSAX* observation Log.

Galaxy	Date	Exposure time[a] (ks)			Count Rate[b] (10^{-2} ct/s)		
		LECS	MECS	PDS	LECS 0.1–4 keV	MECS 1.7–10 keV	PDS 13–30 keV
Sombrero	2000 Jun. 29	23.635	72.087	32.759	1.66 ± 0.11	2.82 ± 0.08	4.32 ± 1.35
NGC 4736	2000 Dec. 29	24.356	76.182	34.677	1.55 ± 0.09	2.29 ± 0.06	

[a] On-source net exposure time. The LECS exposure time is considerably shorter than the MECS one, because the LECS can operate only when the spacecraft is not illuminated by the Sun.
[b] Background subtracted count rates, with photon counting statistics errors, from extraction radii of $6'$ for Sombrero [with the bright G0 star (Sect. 2.1) removed] and $4'$ for NGC 4736.

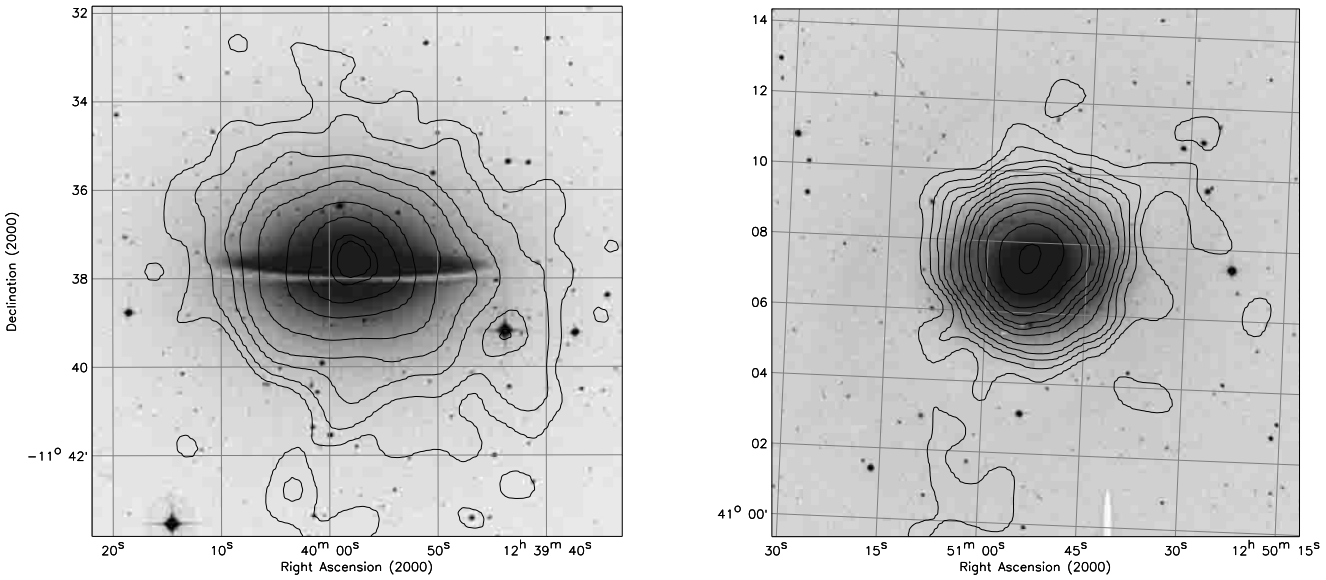

Fig. 1. The MECS image of Sombrero (left) and NGC 4736 (right) in the 2–10 keV band, smoothed with a gaussian of $\sigma = 24''$. Contour levels represent the 8, 10, 15, 20, 30, 50, 70, 90 and 95% of the peak intensity (left), and 6, 8, 10, 12, 15, 20, 25, 30, 40, 50, 70 and 95% of it (right). The contours are overlaid on the DSS image of the Space Telescope Science Institute.

files accumulated on different pointings of empty fields[2]. Figures 2 and 3 show that the source emission becomes comparable to the background level at radii of $\sim5-6'$ for Sombrero and $\sim3-4'$ for NGC 4736. The hard emission is clearly extended in Sombrero relative to the instrumental PSF, while a less significant excess is seen in NGC 4736

[2] These files are those released in Nov. 1998 for the MECS and Dec. 1999 for the LECS. A comparison of the background emission estimated from the field of the galaxies (in a region far from sources) with that estimated from the blank fields (in the same region, in detector coordinates) shows that the two estimates agree within 5% for the MECS and 1% for the LECS.

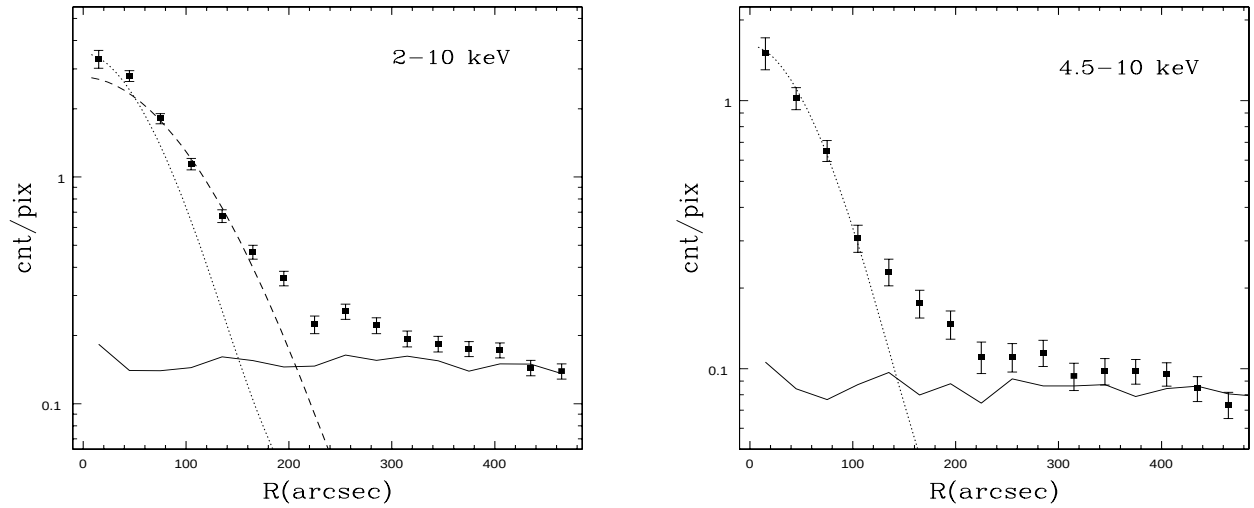

Fig. 2. The MECS 2–10 and 4.5–10 keV radial profiles of the total (squares) and background (solid line) emission from Sombrero. Also shown is the PSF profile of 2 (dashed line) and 5 keV (dotted line) photons. A circular region of 32″ radius centered on the G0 star was omitted.

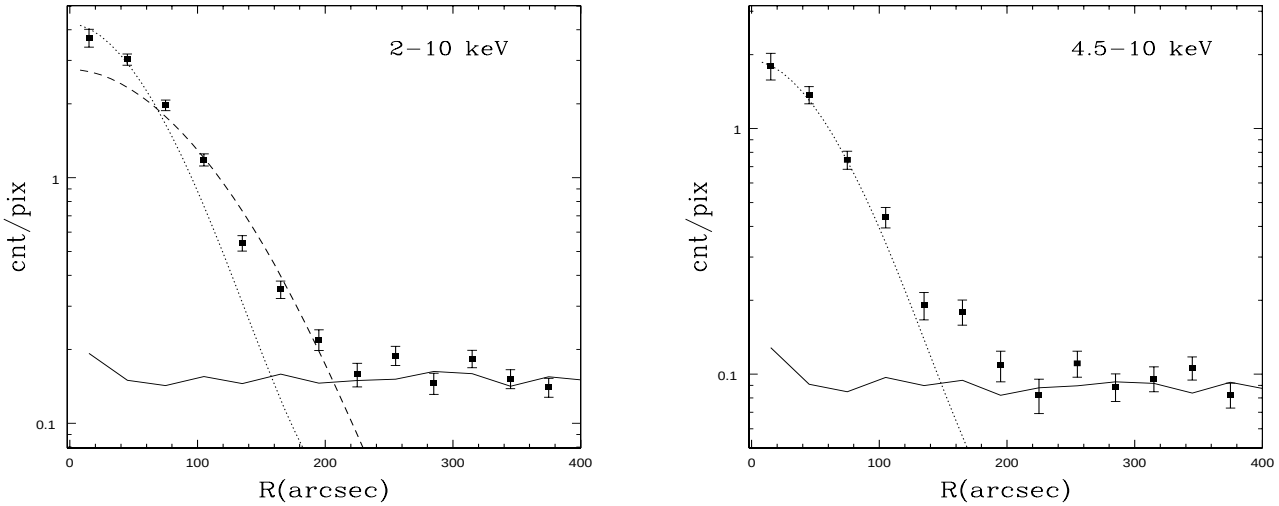

Fig. 3. The MECS 2–10 and 4.5–10 keV profiles of the total (squares) and background (solid line) emission from NGC 4736. Dashed and dotted lines represent the 2 and 5 keV PSF profiles.

Table 3. *Chandra* ACIS-S observation Log.

Galaxy	Obs. ID	Date	Exp.[a]	Chip	Sub.[b]
Sombrero	407	1999 Dec. 12	1.766	7 (S3)	1/8
NGC 4736	808	2000 May 13	47.37	7 (S3)	1/4

[a] On-source net exposure time in ks.
[b] Subarray mode used to reduce pile-up.

above 4 keV. In order to reassure ourselves that the angular extension is not produced by the presence of the star in Sombrero, we derived radial profiles in four azimuthal sectors positioned along the north-south and east-west axes. The same conclusions as before are drawn.

The background-subtracted PDS count rate toward the Sombrero galaxy is $(4.32 \pm 1.35) \times 10^{-2}$ counts s^{-1} in the 13–30 keV band. This corresponds to a $\gtrsim 3\sigma$ detection. We have checked for any possible contaminants in a region of 2 degrees radius around Sombrero using the *ASCA* SIS and GIS and $HEAO-1$ Source Catalogs; we found no catalogued and bright hard X-ray sources. Of course it is possible that both faint unknown hard X-ray sources and small systematic errors in the background subtraction (Guainazzi & Matteuzzi 1997) contribute to the observed PDS count rate. For this reason we consider this detection tentative. It must be confirmed by hard X-ray imaging observations. NGC 4736 was not detected by the PDS instrument; the net 13–30 keV count rate is $(1.8 \pm 1.3) \times 10^{-2}$ counts s^{-1}.

2.2. Chandra observations

The journal of the *Chandra* ACIS-S observations (Weisskopf et al. 1996) is given in Table 3. We used Level 2

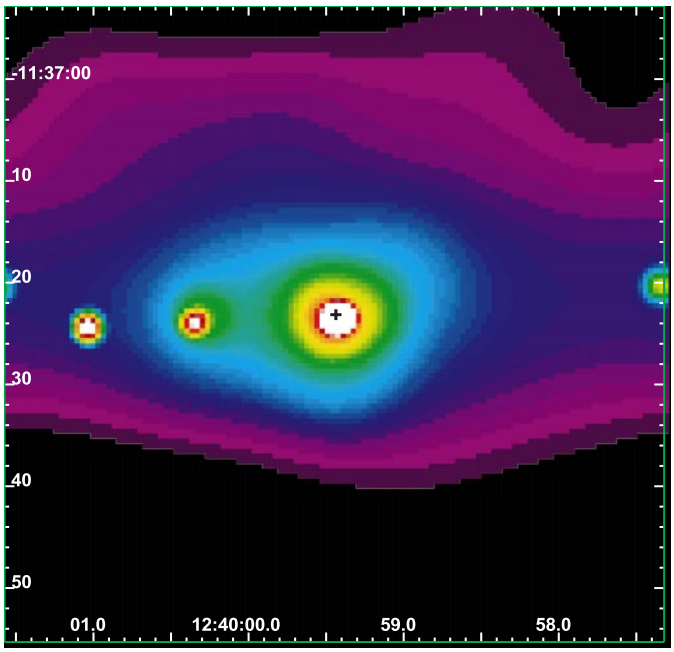

Fig. 4. The central $1' \times 1'$ portion of the ACIS-S image of Sombrero in the 0.3–7 keV band, adaptively smoothed with gaussians of σ ranging from $0''.5$ to $64''$. An unresolved radio source detected with the VLA at 8.4 GHz (Thean et al. 2000) is shown with a cross.

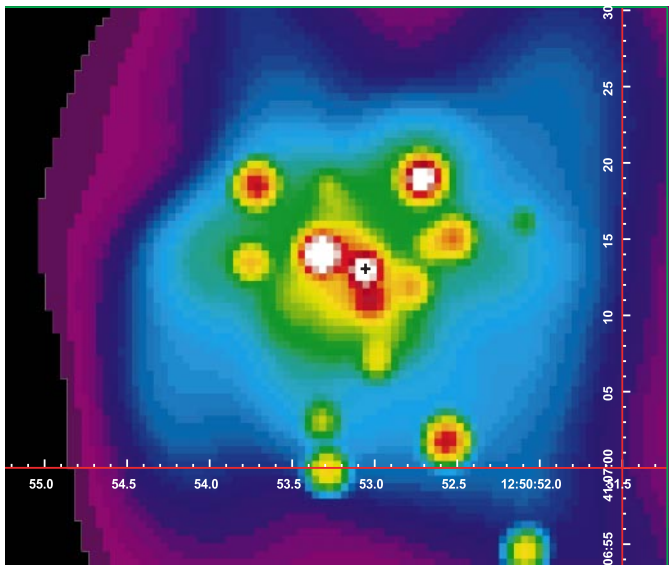

Fig. 5. The central $0'.5 \times 0'.5$ portion of the ACIS-S image of NGC 4736 in the 0.3–7 keV band, adaptively smoothed with gaussians of σ ranging from $0''.5$ to $64''$. The compact nuclear source detected with the VLA (Turner & Ho 1994) is shown with a cross. The bright source north-east of this X-ray/radio source is the brightest of the field.

reprocessed archived event files produced at the *Chandra* X-ray Center (CXC). The 0.3–7 keV images of the central region of the pointed fields are shown in Figs. 4 and 5, where the data were adaptively smoothed with the CXC CIAO tool csmooth. The positions of two compact radio sources detected with the VLA in the nuclear regions are also marked; absolute positional accuracy for these sources are $<0''.5$ for NGC 4736 and $0''.25$ for Sombrero, while the *Chandra* aspect solution is currently limited by systematics to $\sim 0''.5$ accuracy (Aldcroft et al. 2000).

Both the image (Fig. 4) and the radial profiles (Fig. 6) of Sombrero indicate the presence of a bright and hard central point source, coincident with the radio nuclear source, plus extended emission. This becomes clearly visible at radii of $2''-3''$ in the 0.3–7 keV band and at $\sim 6''$ in the 1–7 keV band (from the comparison with the *Chandra* PSF, Fig. 6). Therefore soft emission, most likely coming from hot gas and/or soft binaries (see Sect. 5.1), gives a non-negligible contribution down to the very central region. The present data do not allow a reliable assessment of its the shape and level due to the very short exposure time.

At variance with Sombrero, various point sources are visible at the center of NGC 4736, embedded within a bright diffuse emission region. Moreover, the compact nuclear radio source does not coincide with the brightest X-ray source, but with a much fainter one (Fig. 5). The surface brightness profiles in the same physical region (the central ~ 1 kpc) of Sombrero and NGC 4736 are compared in Fig. 7. This comparison is aimed at showing the two galaxies as if they were at the same distance from us, in the hard band. Before calculating its profile, we blurred the image of NGC 4736 to a lower angular resolution (to compensate for the smaller distance) and we considered only data corresponding to a net exposure time equal to that for Sombrero (extracted from the center of the exposure interval). Figure 7 reveals that the profile of NGC 4736 is less smooth than that of Sombrero, due to the presence of hard and bright individual sources, and lacks a dominating central point source.

3. Spectral analysis

We investigated the spectral properties of the entire galaxies, using *BeppoSAX* data, and of the central point sources, using *Chandra* data. With the latter we also studied the overall spectral shape of the largest central portion of the galaxies that was observed (more details below) *just to check the consistency with the global BeppoSAX results*. The LECS and MECS background spectra were estimated from the same blank fields used in Sect. 2.1; RMF and ARF files released in September 1997 were used. The analysis of the LECS and MECS spectra was done over 0.1–4 keV and 1.7–10 keV respectively. We fitted the models simultaneously to the LECS and MECS data, and then we considered the PDS ones in the case of Sombrero. In the fitting a normalization constant was introduced to allow for known differences in the absolute cross-calibrations between the detectors (Fiore et al. 1999). For the ACIS-S data, RMF and ARF files for the source and background spectra were created using the script "psextract" in the CIAO 2.1.2 software and the *Chandra* CALDB version 2.6. We derived the background locally as detailed below. Finally, source counts

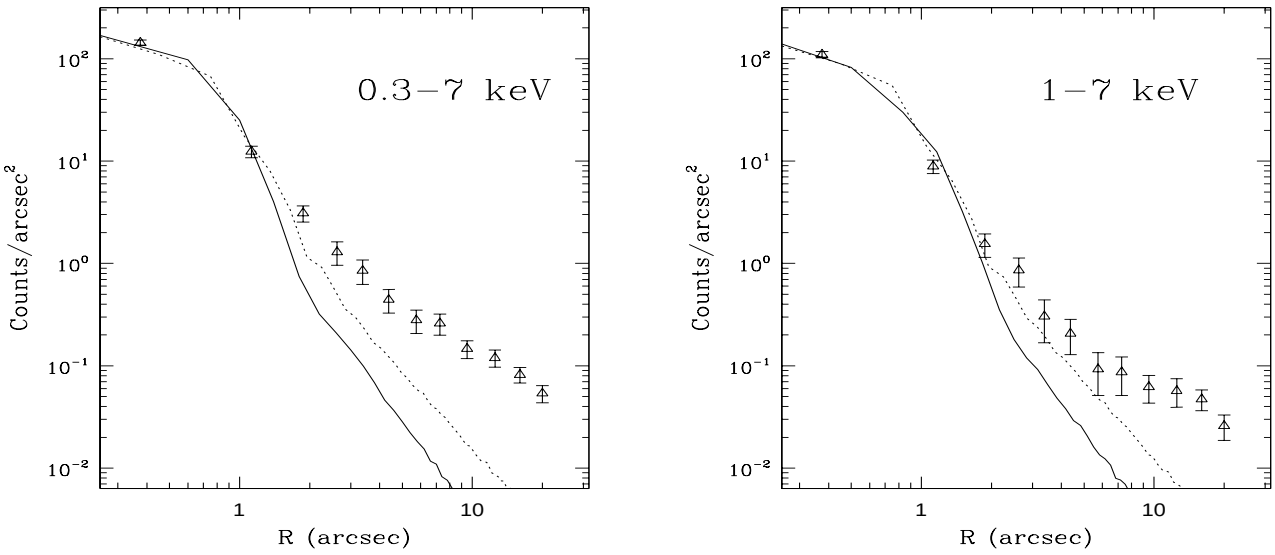

Fig. 6. The ACIS-S radial profile of the center of Sombrero (triangles) in the 0.3–7 keV and 1–7 keV bands, together with the PSF profiles for 5 keV (dotted line), 0.8 keV (solid line, left panel) and 1 keV (solid line, right panel). The PSF was estimated from the standard *Chandra* PSF library files for the source location in the telescope field of view. The bright source ∼20″ east of the nucleus (Fig. 4) was removed from the calculation.

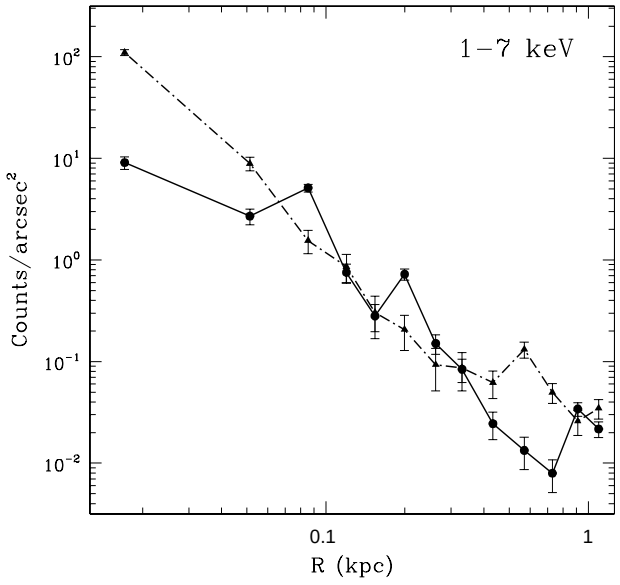

Fig. 7. The central 1–7 keV brightness profiles of Sombrero (dot-dashed line) and NGC 4736 (solid line), from ACIS-S data. The Sombrero profile is the same as in Fig. 6, except that no source was removed from the calculation. The NGC 4736 profile, centered on the radio nucleus, comes from an image adapted from the original one, as detailed at the end of Sect. 2.2.

were rebinned to obtain at least 20 counts per energy channel. Spectral fits were performed using XSPEC (version 11.0.1). Quoted errors on the fit parameters or upper limits refer to the 90% confidence interval for one interesting parameter ($\Delta\chi^2 = 2.71$).

Table 4. Sombrero – results of the LECS and MECS spectral analysis.

Power law model:	
$N_{\rm H}$ (10^{20} cm^{-2})	1.2 (0–5.8)
Γ	1.85 (1.74–1.97)
Flux (10^{-12} erg cm^{-2} s^{-1})	1.5, 2.0
Lum (10^{40} erg s^{-1})	2.5, 2.1
χ^2/ν	103/113
Power law + Mekal model ($Z = 0.5\ Z_\odot$):	
$N_{\rm H}$ (10^{20} cm^{-2})	31 (2–70)
Γ	1.95 (1.87–2.15)
Flux (10^{-12} erg cm^{-2} s^{-1})	0.7, 2.0
Lum (10^{40} erg s^{-1})	3.1, 2.1
kT(keV)	0.3 (0.2–0.5)
Flux (10^{-12} erg cm^{-2} s^{-1})	0.6, 0.
Lum (10^{40} erg s^{-1})	0.9, 0.
χ^2/ν	98/111

$N_{\rm H}$ is the column density of neutral hydrogen in addition to $N_{\rm H,Gal}$ given in Table 1. Values between parentheses give the 90% confidence interval. ν is the number of degrees of freedom of the fit. Observed fluxes and intrinsic luminosities are given in the 0.1–2 and 2–10 keV bands.

3.1. Sombrero

3.1.1. Analysis of BeppoSAX data

The spectral counts, extracted from a circle of 6′ radius (Sect. 2.1), are well fitted by a simple power law of $\Gamma \sim 1.8$ with $N_{\rm H}$ consistent with the Galactic value (Fig. 8, Table 4). The PDS data fall well above this model (in Fig. 8 the normalization constant between the MECS and the PDS fluxes was fixed at its canonical value). We

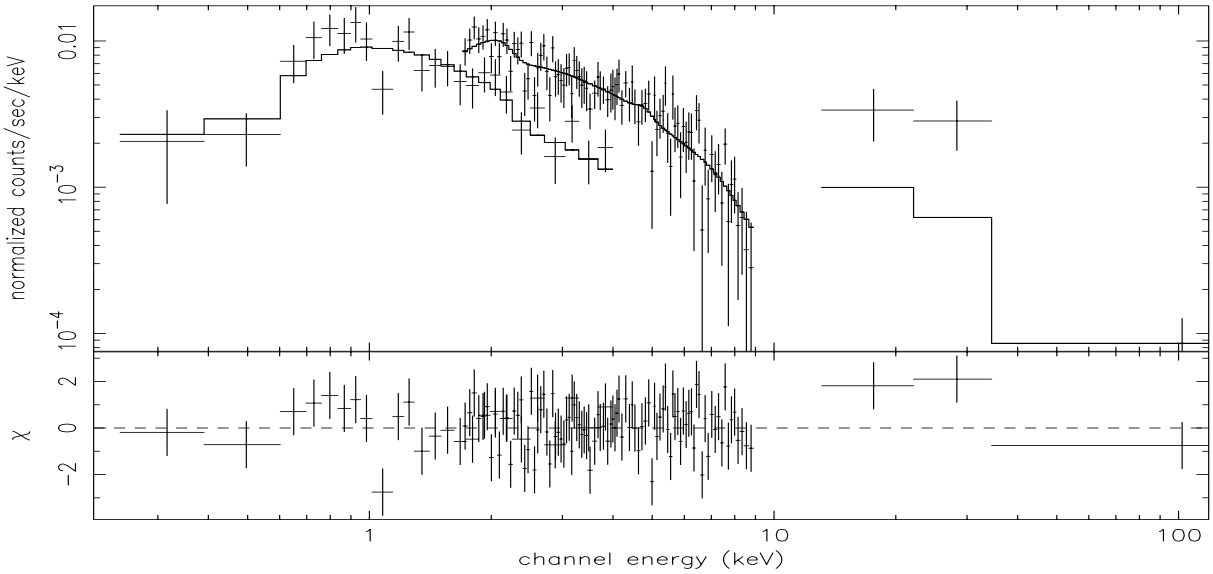

Fig. 8. The LECS, MECS and PDS spectra of Sombrero together with their modeling with a power law (Sect. 3.1.1, Table 4). Folded spectra and residuals are shown.

Table 5. Spectral results from ACIS-S data for central point sources.

Power law model:	Sombrero nucleus	NGC 4736 radio nucleus[a]	NGC 4736 brightest source
$N_{\rm H}$ (10^{20} cm^{-2})	17 (8–28)	27 (7-66)	<1.5
Γ	1.5 (1.2–1.9)	1.9 (1.8–2.2)	1.22 (1.19–1.29)
Flux (10^{-12} erg cm^{-2} s^{-1})	1.6	0.2	0.7
Lum (10^{39} erg s^{-1})	17	0.6	3.0
χ^2/ν	0.68	0.98	0.89

The $N_{\rm H}$ value is in addition to $N_{\rm H,Gal}$ in Table 1. Values between parentheses give the 90% confidence interval. Observed fluxes and intrinsic luminosities refer to the 2–10 keV band.
[a] A thermal component was added to the power law (Sect. 3.2.2).

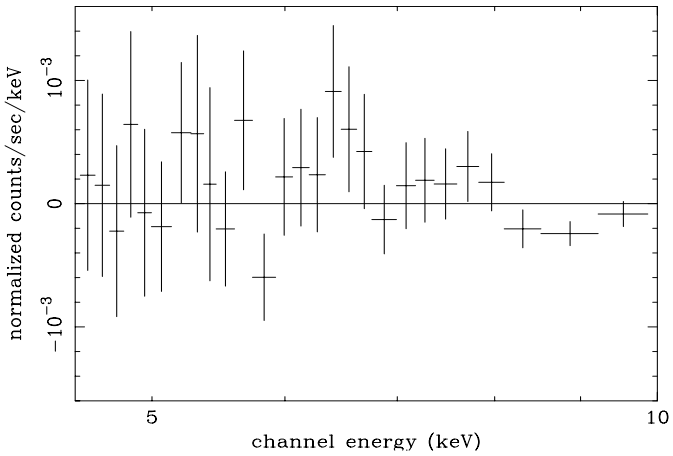

Fig. 9. The residuals between the MECS spectrum of Sombrero extracted from the central 3′ and a simple power law model, around the 6.5 keV "emission line" (Sect. 3.1.1).

could not reproduce this excess by adding a highly absorbed power law. Since there are no catalogued bright hard sources in the PDS field of view (Sect. 2.1), nor is any visible in the MECS, an unknown source could be producing the excess. Its 13–30 keV flux would be $>2.5\times10^{-12}$ erg cm^{-2} s^{-1} when extrapolating the best fit MECS power law into the PDS energy range and comparing the expected with the observed count rate (considering also the PDS response outside the MECS field of view).

The addition of a soft thermal component (a MEKAL model) improves the fit quality, but is significant at 95% confidence level only, according to the F-test. Its best fit temperature is $kT\sim0.3$ keV, its abundance is not constrained, and its presence requires an intrinsic absorption to the power law component of $N_{\rm H,intr}=3.1\times10^{21}$ cm^{-2} at the best fit (Table 4).

We also studied the MECS spectrum extracted from a circle of 3′ radius to investigate the hard spectral properties of an emission region that is more dominated by the nuclear emission. In this case an emission line is found at $6.50^{+0.20}_{-0.21}$ keV of equivalent width 291^{+205}_{-226} eV (Fig. 9). The evidence for it is marginal, though, since it is

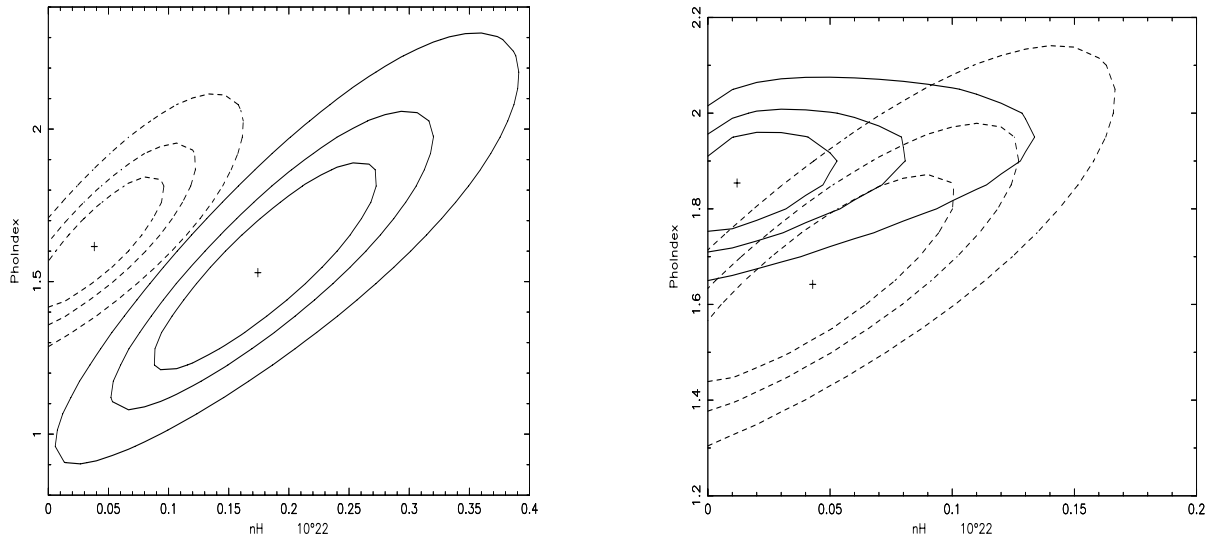

Fig. 10. The 68%, 90% and 99% confidence contours for Γ and $N_{\rm H,intr}$ derived for Sombrero (Sects. 3.1.1 and 3.1.2). Dashed contours refer to the ACIS-S spectrum extracted from a $0.'5$ radius; solid contours refer to the ACIS-S spectrum from a $2''$ radius in the left panel, and the LECS+MECS spectrum in the right panel.

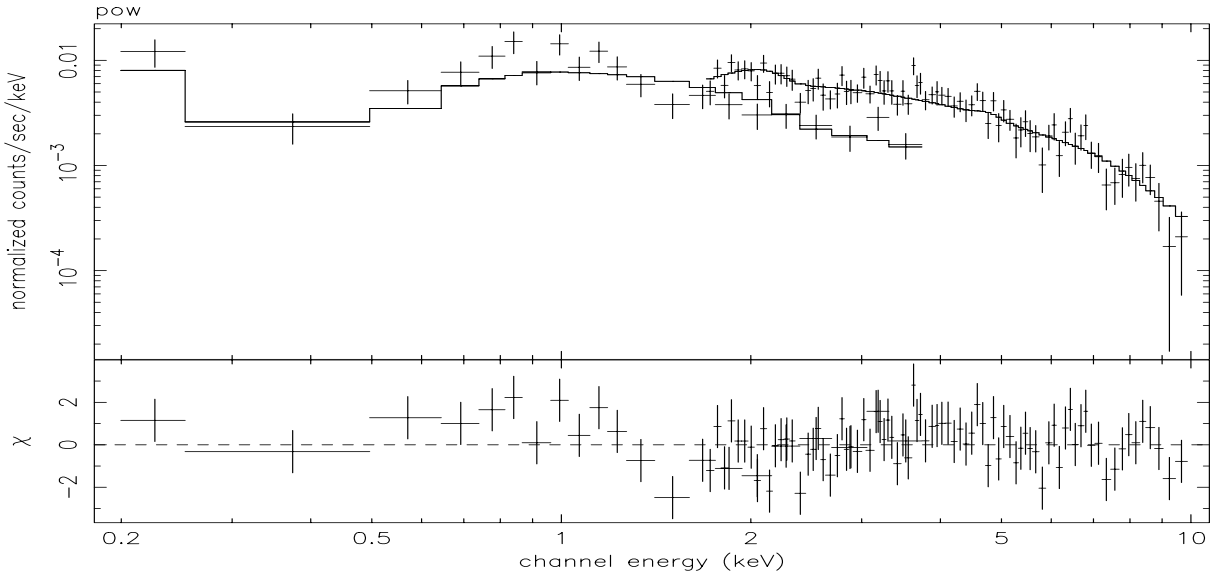

Fig. 11. The LECS and MECS spectra of NGC 4736 fitted with a power law (Table 6). Folded spectra and residuals are shown.

statistically significant at 93% confidence only, according to the F-test.

3.1.2. Analysis of *Chandra* data

We studied the ACIS-S spectra of a central region of $2''$ radius, where the emission from the central point source dominates (Fig. 6), and from the largest accessible region of the galaxy (this observation was performed in subarray mode), i.e., a circle of $0.'5$ radius. The background of the first spectrum was derived locally, from an annulus of inner and outer radii of $5''$ and $9''$. That of the $0.'5$ spectrum comes from a circle of $25''$ radius located as far as possible from the center of the galaxy (in the north direction) but still within the S3 chip. The spectral fits were performed over 0.5–5 keV, because not enough counts were detected above 5 keV. The spectra are well described by simple power laws, whose $\Gamma \sim 1.5$ and 1.6 at the best fit, respectively for the small and the large extraction region (Table 5). The uncertainties on the spectral parameters are large, due to the short exposure time (Fig. 10, left panel). Taking the extreme values on the 90% confidence contour in this figure, the 2–10 keV observed flux of the central spectrum ranges from 1.1×10^{-12} to 2.2×10^{-12} erg cm^{-2} s^{-1} [and its $L(2-10\,\mathrm{keV}) = (1.2-2.3)\times10^{40}\,\mathrm{erg\,s^{-1}}$]. In the 0.5–5 keV band, the $2''$ radius region contributes ∼60% of the counts from the $0.'5$ one; in the 2–10 keV band it contributes ∼70% of them. At least one clear difference between the two spectra is found (Fig. 10, left panel): the central one requires an absorption in excess of the Galactic value, while the spectrum from $0.'5$ does not. This result is in

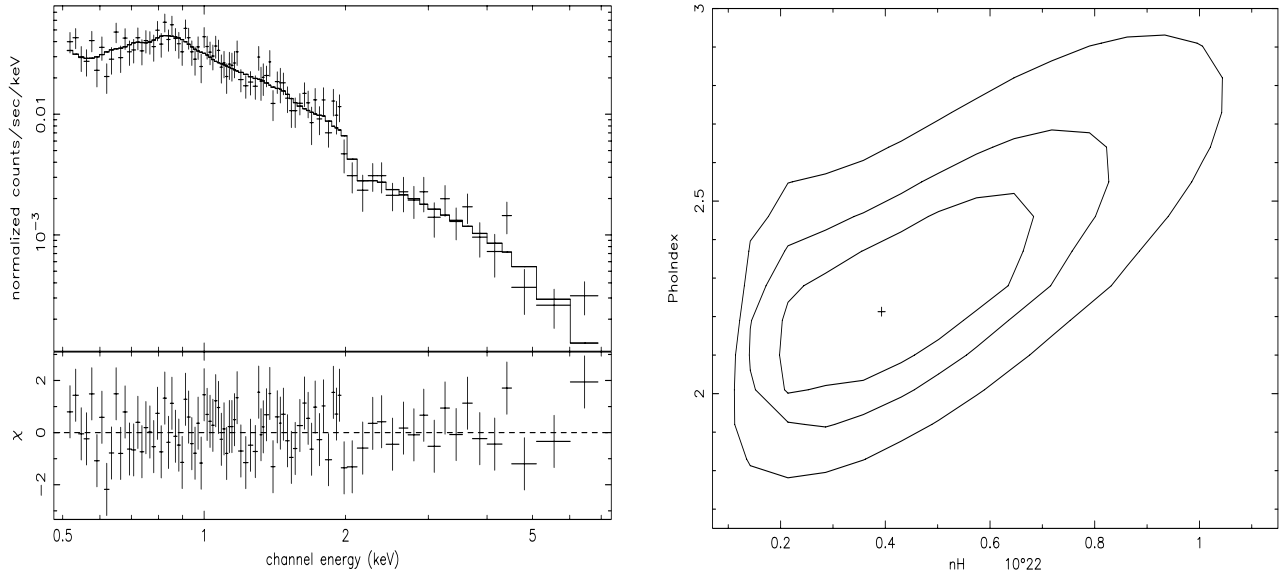

Fig. 12. Left: the ACIS-S spectrum of the X-ray/radio point source in NGC 4736, fitted with a power law plus a thermal component (Sect. 3.2.2). Right: 68, 90 and 99% confidence contours for the parameters $N_{\rm H,intr}$ and Γ describing the model on the left.

Table 6. NGC 4736 – Results of the LECS and MECS spectral analysis.

Power law model:	
$N_{\rm H}$ (10^{20} cm^{-2})	0.0 (<0.7)
Γ	1.69 (1.60–1.78)
Flux (10^{-12} erg cm^{-2} s^{-1})	1.3, 1.9
Lum (10^{39} erg s^{-1})	7.0, 7.7
χ^2/ν	112/97
Power law + Mekal model ($Z = Z_\odot$):	
$N_{\rm H}$ (10^{20} cm^{-2})	0 (<1.4)
Γ	1.63 (1.52–1.71)
Flux (10^{-12} erg cm^{-2} s^{-1})	1.2, 1.9
Lum (10^{39} erg s^{-1})	6.2, 7.9
kT(keV)	0.3 (0.2–0.6)
Flux (10^{-12} erg cm^{-2} s^{-1})	0.4, 0.
Lum (10^{39} erg s^{-1})	1.9, 0.
χ^2/ν	99/95

$N_{\rm H}$ is the column density of neutral hydrogen in addition to $N_{\rm H,Gal}$ given in Table 1. Values between parentheses give the 90% confidence interval. ν is the number of degrees of freedom of the fit. Observed fluxes and intrinsic luminosities are given in the 0.1–2 and 2–10 keV bands.

agreement with the absence of intrinsic absorption found from *BeppoSAX* data. Figure 10 (right panel) also shows some overlap between the spectral results obtained from the LECS+MECS data for the whole galaxy and those obtained for the 0′.5 radius region from ACIS-S data. The Γ value given by *BeppoSAX* tends to be larger, though, as if the galactic emission were softer than that of the central region. This is in accordance with the steepening of the power law slope found by FJ from *ROSAT* PSPC data when increasing the extraction radius (Sect. 1.1). In the 0′.5 ACIS-S spectrum there is no significant evidence for a soft thermal component, however the data uncertainties are large.

3.2. NGC 4736

3.2.1. Analysis of BeppoSAX data

Spectral counts were extracted from a circle of 4′ radius (Sect. 2.1). Their fit with a simple power law is of poorer quality than for Sombrero (Table 6), mostly because this model leaves an excess of emission around 1 keV (Fig. 11). The addition of a thermal component of $kT \sim 1$ keV and extremely low abundance improves significantly the quality of the fit, but this model is not realistic. Moreover, this soft component largely dominates the observed emission below 2 keV, because the power law becomes highly absorbed ($N_{\rm H,intr} > 2 \times 10^{22}$ cm^{-2}), in contrast with what found from *ROSAT* data (Sect. 1.1). The abundance is not constrained by the LECS data, though, and if we fix it at any $Z \gtrsim 0.1\ Z_\odot$, any intrinsic $N_{\rm H}$ to the power law is $<1.4 \times 10^{20}$cm^{-2}, while the addition of the thermal component still gives a significant improvement ($Z = Z_\odot$ in Table 6; if $Z = 0.1\ Z_\odot$, the values of kT and Γ are still within the uncertainties in Table 6). The addition of a second soft thermal component does not improve the fit quality further. No emission lines at high energies are detected; the equivalent width of any Fe-K emission at 6.4 or 6.7 keV is <380 eV and <420 eV respectively.

3.2.2. Analysis of *Chandra* data

We studied the spectra of two point sources in the nuclear region: the brightest one, which is also the brightest of the field, and the one coincident with the nuclear radio source

(Fig. 5). We extracted counts from a circle of 1.″5 radius and we used as background a circle of 5.″5 radius, centered on the X-ray/radio point source, from which we removed the point sources lying within. We also studied the spectral shape of the largest accessible portion of the galaxy, a circle of 55″ radius, for which the background was taken from a circle of 50″ radius, located as far as possible from the center of NGC 4736 but still within the S3 chip. The spectral fits were performed over the 0.5–7 keV range.

Both point sources can be modeled by power law spectra, however with significantly different parameters (Table 5): the brightest one has $\Gamma = 1.22$ without intrinsic absorption, the X-ray/radio point source is softer and absorbed (Fig. 12). Moreover, the addition of a soft thermal component gives a significant improvement of the fit of this source. Since it is embedded in a diffuse emission region (Fig. 5), we checked whether a "pure" source spectra could be obtained by restricting further the extraction radius and by using various alternative background estimates (i.e., obtained from a region closer to the point source, or inserting it as a thermal component with free normalization). The fitting results always remained very similar. If we adopt the 1.″5 source extraction radius and a thermal model for the the background, then $\Gamma \sim 1.9$ for the power law component (Table 5), and $kT = 0.65^{+0.05}_{-0.06}$ keV, $Z = 0.07^{+0.27}_{-0.01}\ Z_\odot$ for the thermal component. We also tried to reproduce the softer part of the spectrum with a multicolor disk blackbody emission, in addition to a power law, which is the usual modeling adopted for black hole binaries (Tanaka & Shibazaki 1996). The quality of the fit improves with respect to that with a simple power law, but is not as good as when a thermal component is added.

The "global" galaxy spectrum requires at least two thermal components plus a power law one (of $\Gamma = 1.47^{+0.04}_{-0.05}$) without intrinsic absorption. The two temperatures are $kT = 0.23^{+0.13}_{-0.04}$ keV (with $Z = 0.02\ Z_\odot$ at the best fit, and $Z < 1.6\ Z_\odot$) and $kT = 0.57^{+0.01}_{-0.02}$ keV (with $Z = 0.8\ Z_\odot$ at the best fit, and $Z > 0.2\ Z_\odot$). When constraining the abundances to be the same, their common value becomes $Z = 0.24^{+0.27}_{-0.08}\ Z_\odot$ (the other spectral parameters remain practically unchanged). Note that these "global" fit results are only preliminary, awaiting for improved soft-band calibration of ACIS-S. The *BeppoSAX* and the "global" *Chandra* spectra give consistent photon index values. At lower energies, the higher sensitivity and spectral resolution of ACIS-S can distinguish the presence of two thermal components.

4. Variability

Given the complexity of the sources considered, a variability study with low angular resolution data is clearly limited. For a comparison with previous analyses, though, we use the *BeppoSAX* data to study the short and long term variability.

ROSAT HRI data showed that the nuclear source in Sombrero might be time variable (FJ). To investigate this point we extracted the 2–4 keV, 4–10 keV and 2–10 keV light curves for the MECS count rates of the central 3′ radius circle. Just a hint of variability was found. A χ^2 test on the 2–10 keV data, to quantify how the observed count rate differs from a constant average emission, gives a probability of chance occurrence of ∼80%. So, the "nuclear" emission does not show a statistically significant variation on the time scales sampled here. *ROSAT* and *ASCA* data do not show evidence of significant short term temporal variability for NGC 4736 (R99), and the same is found from the 2–10 keV MECS data. In conclusion, for both galaxies we can at least exclude variations of the 2–10 keV flux larger than ∼50% on time scales of the order of one day.

The sources are stable also in the long term. *ASCA* and *BeppoSAX* 2–10 keV fluxes for Sombrero are consistent with each other (2.2 and 2.0×10^{-12} erg cm^{-2} s^{-1} respectively, pointings made during 1994 and 2000). NGC 4736 showed roughly the same 2–10 keV flux during the *ASCA* and *BeppoSAX* pointings in the years 1995 and 2000 (1.8 and 1.9×10^{-12} erg cm^{-2} s^{-1} respectively). R99 also found the hard continuum level unchanged between the *ROSAT* PSPC and *ASCA* pointings (separated by four years).

5. Summary and discussion

5.1. Sombrero

The main findings derived here are:
1) The hard (>2 keV) MECS emission is extended, consequently it has a non-negligible contribution from distributed sources (e.g., XRBs).
2) A simple power law ($\Gamma \sim 1.8$) without absorption in excess of the Galactic value reproduces well the LECS+MECS spectrum. The addition of soft thermal emission ($kT \sim 0.3$ keV) improves the spectral fit, but is not strictly required.
3) At the galactic center a short ACIS-S exposure shows a single bright and hard source plus additional soft extended emission.
4) The ACIS-S spectra of the nucleus and of a central circle of 0.′5 radius can both be described by simple power laws. The nucleus requires absorption intrinsic to Sombrero, while the larger region does not, in agreement with the *BeppoSAX* result.
5) An emission line consistent with fluorescence from cold iron is marginally detected only in the MECS spectrum of the central 3′ circle, so (if real) it could originate in the nucleus. The statistics of ACIS-S data above 5 keV are too low to investigate this point.
6) No significant short or long term flux variability is found.

Below we discuss the global galaxy X-ray properties and then (Sect. 5.2) we consider the possibility of the presence of a low luminosity AGN (LLAGN).

Soft thermal emission is indicated by the *BeppoSAX* spectrum and by the ACIS-S 0.3–7 keV brightness profile.

Its origin is likely due to hot gas and/or stellar sources with soft emission distributed over the galaxy [see, e.g., those discussed in Pellegrini & Fabbiano (1994), or black hole binaries (Tanaka & Shibazaki 1996)]. The presence of some hot gas in this bulge-dominated galaxy is plausible. The temperature and luminosity of the soft component (Table 4) agree with those expected for the stellar mass losses that can be retained by potential wells of the shape and depth of the Sombrero galaxy (D'Ercole & Ciotti 1998). The central stellar velocity dispersion of the bulge ($\sigma = 249$ km s^{-1}, McElroy 1995) corresponds to a central gas virial temperature of 0.37 keV, close to the global value found here ($kT = 0.3$ keV). The diffuse emission estimated from the HRI data, including possible truly diffuse gas and unresolved sources, is $L(0.1{-}2.4\text{ keV}) \sim 1.2 \times 10^{40}$ erg s^{-1}(FJ, rescaled for the distance adopted here), consistent with $L(0.1{-}2.4\text{ keV}) \sim 0.9{\times}10^{40}$ erg s^{-1} derived from *BeppoSAX* data for the soft thermal emission.

The global galactic emission in the hard band is largely contaminated by the nuclear source. From ACIS-S data (Sect. 3.1.2), this source contributes $\gtrsim$55% of the MECS 2–10 keV galactic flux. Given that the latter is extended (Fig. 2), there must be some hard emission in excess of the nuclear one, likely due to XRBs. By subtracting the ACIS-S nuclear emission from the *BeppoSAX* spectrum, the hard XRB's contribution is $L(2{-}10\text{ keV}) \lesssim 9 \times 10^{39}$ erg s^{-1}. This upper limit is very close to the XRB's contribution in Sombrero estimated from the best fit $L_{\rm X} - L_{\rm B}$ relation (converted to the 2–10 keV band) of normal spiral galaxies, based on *Einstein* data [i.e., $L(2{-}10\text{ keV}) = 8.7 \times 10^{39}$ erg s^{-1}; Fabbiano et al. 1992]. It is also in agreement with the estimate ($\sim 4{\times}10^{39}$ erg s^{-1}, when converted to the 2–10 keV band) from the $L_{\rm X} - L_{\rm B}$ relation for the collective emission of discrete non-nuclear X-ray sources in spirals, derived recently from a large sample of nearby galaxies observed with the *ROSAT* HRI (Roberts & Warwick 2000).

5.2. The low luminosity AGN in Sombrero

ACIS-S reveals a nuclear spike of $L(2{-}10\text{ keV}){=}(1.2{-}2.3){\times}10^{40}$ erg s^{-1}, whose spectrum is well modeled by an absorbed power law. The small amount of absorption [$N_{\rm H,intr}{=}(0.8{-}2.8){\times}10^{21}$ cm^{-2}] could be explained by intervening dust along the line of sight to the center. An *HST* $V-I$ image, in fact, shows that the nucleus is partially hidden by a dusty environment (Pogge et al. 2000), for which Emsellem & Ferruit (2000) derive $A_V = 0.5$ mag (i.e., $N_{\rm H,intr} = 8.3{\times}10^{20}$ cm^{-2}, for the Galactic extinction law).

Within the uncertainties, still large, the spectral characteristics are consistent with both Seyfert galaxies (Nandra et al. 1997) and XRBs. Could a few bright XRBs be at the origin of the nuclear emission and not be resolved by ACIS-S? This hypothesis requires the presence of hard stellar sources in larger number and/or of higher luminosity than in NGC 4736, within a radius of $\sim$100 pc from the center of Sombrero (e.g., Fig. 7). This seems unlikely, given that it would imply a recent starburst activity, at least as vigorous as in NGC 4736 (Sects. 1.1 and 5.3), for which there is no evidence. Therefore, the possibility of the presence of a LLAGN is more viable. This also ties up with observational results outside the X-ray band, i.e., with the indications for the presence of a central supermassive black hole, of weak optical activity, of compact radio and UV emissions, and also of a faint broad Hα component (Sect. 1.1).

What kind of physical mechanism could be at the origin of the nuclear emission? Its L(2–10 keV) derived here and the Hα luminosity estimate from the spectroscopic survey of Ho et al. (1997) put this nucleus very close to the extension down to low luminosities of the $L_{\rm X} - L_{\rm H\alpha}$ correlation found for powerful Seyfert 1 nuclei and quasars (Ward et al. 1988; Ho et al. 2001). This indicates that the optical emission line spectrum could be powered by photoionization from the central continuum, as in high luminosity AGNs. This nucleus could then behave like a downsized version of a bright AGN, a possibility investigated more in detail for the LLAGN in NGC 4258 by Fiore et al. (2001). Support for this interpretation could also come from the possible presence of a $\sim$6.4 keV emission line in the MECS spectrum (Sect. 3.1.1), as often observed in Seyfert galaxies (Nandra et al. 1997). Its equivalent width is similar to that of type 1 AGNs, while stronger lines are usually found in type 2 AGNs, consistent with the fact that large absorption is not required by our spectral analysis.

A detailed study and modeling of the global spectral energy distribution (SED) of the nuclear emission is beyond the scope of this work. We just note that this SED differs from the canonical broadband continuum of bright AGNs in the lack of an ultraviolet excess (Nicholson et al. 1998), a property common to a few LLAGNs (Ho 1999, who also argues that it is not an artifact of dust extinction). This finding, together with the highly sub-Eddington regime of accretion onto the central massive black hole[3], has encouraged the developement of advection dominated accretion flow (ADAF) models for LLAGNs (Quataert et al. 1999). Recent modifications of the standard ADAF model including outflows or convection (Narayan et al. 2000) allow the luminosity to be further reduced and have been recently advocated to explain the very low *Chandra* upper limits on the nuclear emission in three giant elliptical galaxies (Loewenstein et al. 2001).

5.3. NGC 4736

From our analysis it turns out that:
1) The LECS and MECS spectra require a hard component (a power law of $\Gamma \sim 1.6$), a soft thermal component ($kT = 0.2 - 0.6$ keV) contributing $\lesssim$30% of the total

[3] The *Chandra* measurement of the nuclear 2–10 keV luminosity (Sect. 3.1.2) together with the black hole mass estimate of Kormendy et al. (1996) give $L_{\rm X} \sim 10^{-7} L_{\rm Edd}$.

observed flux below 2 keV, and absorption consistent with the Galactic value. The ACIS-S spectrum of the central $\sim 1'$ radius region requires a two temperature fit for the soft thermal component.
2) No Fe-K emission line is found superimposed on the hard continuum. No short or long term flux variability is detected.
3) The ACIS-S image reveals a cluster of at least four bright point sources within the central circle of $5''$ radius, embedded in diffuse emission. The brightest source has $L(2-10\ \mathrm{keV}) \sim 3\times10^{39}\ \mathrm{erg\,s^{-1}}$ and $\Gamma \sim 1.2$. So, it is similar to the most luminous [$L(2-10\ \mathrm{keV}) \gtrsim 10^{39}\ \mathrm{erg\,s^{-1}}$] sources discovered with ACIS-S in the starforming regions of the Antennae galaxies (Fabbiano et al. 2001; Zezas et al. 2001). X-ray sources with luminosities equivalent to the entire Eddington luminosity for accretion onto a $(10-10^3)\ M_\odot$ object, recently collectively defined "ultra-luminous X-ray sources" (e.g., Makishima et al. 2000), are preferentially found in starforming regions. For them, mild X-ray beaming during a short but common stage in the evolution of intermediate and high mass XRB's has been recently suggested (King et al. 2001).
4) The compact radio nuclear source does not coincide with the brightest X-ray source but with a fainter [$L(2-10\ \mathrm{keV}) \sim 6\times10^{38}\ \mathrm{erg\,s^{-1}}$] and absorbed source. Its spectrum further requires a thermal ($kT = 0.6-0.7$ keV) component, perhaps a local enhancement of hot gas density at the position of this nucleus. The same requirement has been found studying the spectra of a few point sources in the star-forming regions of the Antennae (Fabbiano et al. 2001; Zezas et al. 2001) and of the nuclear source in the Sa galaxy NGC 1291 (Irwin et al. 2001).
5) the 1–7 keV brightness profile looks more clumpy than that of the Sombrero galaxy (due to a larger number of bright XRBs in the central region) and the nuclear point source is much less dominating.

From the present investigation a starburst-induced origin for the LINER activity is clearly preferred. This is based on the X-ray results showing that: 1) the presence of a LLAGN is not conspicuous; 2) there is a large number (at least with respect to the case of Sombrero) of hard and bright point sources at the galactic center, at least two of which have properties similar to those of the Antennae sources (Fabbiano et al. 2001); 3) the total 2–10 keV MECS emission ($\sim 8\times10^{39}\ \mathrm{erg\,s^{-1}}$) is clearly in excess of that expected for hard binaries in normal spirals (this, calculated as in Sect. 5.1, is $3.4\times10^{39}\ \mathrm{erg\,s^{-1}}$ from the Fabbiano et al. relation and $1.1\times10^{39}\ \mathrm{erg\,s^{-1}}$ from the Roberts & Warwick relation), and this is not due to the presence of a bright nucleus, as the ACIS-S image reveals; 4) for the soft thermal emission both *BeppoSAX* and ACIS-S indicate a temperature larger than the gas virial temperature [$\sigma = 136\ \mathrm{km\,s^{-1}}$ for this galaxy (McElroy 1995), that corresponds to $kT \sim 0.1$ keV], a property that can be easily explained with heating of the interstellar gas by the starburst (e.g., Heckman 2000).

Is there some residual evidence in favour of a LLAGN? The brightness temperature of the nuclear radio source suggests the presence of an AGN rather than, e.g., an HII region (Turner & Ho 1994), while the nuclear bright UV point source revealed by *HST* could even be a compact star cluster (Maoz et al. 1995). Unless the X-ray/radio source was in a very faint state during the ACIS-S pointing [at 90% confidence its $L(2-10\ \mathrm{keV}) < 10^{39}\ \mathrm{erg\,s^{-1}}$] this possible AGN is of extremely low luminosity. A central supermassive black hole of $2.2\times10^7\ M_\odot$ is inferred from the $M_{\rm BH}-\sigma$ relation (Ferrarrese & Merritt 2000), from which we derive $L(2-10\ \mathrm{keV})/L_{\rm Edd} \sim 2\times10^{-7}$. Garcia et al. (2000) report a similarly low luminosity X-ray source [$L(0.3-7\ \mathrm{keV}) < 1.6\times10^{38}\ \mathrm{erg\,s^{-1}}$] detected by ACIS-I within $1''$ of the radio nucleus of the M 31 galaxy, which hosts a central compact dark object of $3.0\times10^7\ M_\odot$. This source seems to be much softer (its $\Gamma = 4.5\pm1.5$) than the nuclear X-ray/radio source in NGC 4736, though.

6. Conclusions

We have presented the analysis of the *BeppoSAX* observations of two nearby LINER galaxies, complemented with a study of their central regions based on *Chandra* ACIS-S data. This analysis has shown that 1) the X-ray emission has a different origin in the two galaxies: an AGN in Sombrero and a recent starburst in NGC 4736, which reinforces the evidence that LINERs may represent more than one physical phenomenon, as mentioned in Sect. 1; and 2) hard X-ray data taken at very low angular resolution (such as those that can be obtained by *BeppoSAX* or *ASCA*) can be misleading, and the high resolution imaging spectroscopy provided by *Chandra* is essential to draw conclusions concerning the origin of the LINER activity. Also, the global galactic spectral properties can be very different from those of the nuclear sources, because these do not largely dominate the total emission.

The *BeppoSAX* data indicate the presence of hard and extended emission, in excess of that expected for the collective emission of discrete X-ray sources in spirals, plus soft thermal emission, that is more evident in the spectrum of NGC 4736. The soft emission could plausibly come from hot gas retained by the galactic potential well in Sombrero, and by gas heated by supernovae in NGC 4736. An extremely low luminosity AGN could still be present in NGC 4736, though, due to the presence of a compact non-thermal radio source coincident with an X-ray faint central point source.

Acknowledgements. G. Fabbiano acknowledges support from NASA contract NAS 8-39073 (Chandra X-ray Center) and S. Pellegrini and G. Trinchieri from ASI and MURST.

References

Ajhar, E. A., Lauer, T. R., Tonry, J. L., et al. 1997, AJ, 114, 626
Aldcroft, T., Karovska, M., Cresitello-Dittmar, M., Cameron, R., & Markevitch, M. 2000, Proc. SPIE, 4012, 74
Alonso-Herrero, A., Rieke, M. J., Rieke, G. H., & Shields, J. C. 2000, ApJ, 530, 688

Boella, G., Chiappetti, L., Conti, G., et al. 1997, A&AS, 122, 327
Crane, P., Stiavelli, M., King, I. R., et al. 1993, AJ, 106, 1371
Cui, W., Feldkhun, D., & Braun, R. 1997, ApJ, 477, 693
D'Ercole, A., & Ciotti, L. 1998, ApJ, 494, 535
de Vaucouleurs, G., de Vaucouleurs, A., Corwin, Jr. H. G., et al. 1991, Third Reference Catalogue of Bright Galaxies (Springer Verlag, New York)
Emsellem, E., & Ferruit, P. 2000, A&A, 357, 111
Eracleous, M., Shields, J. C., Chartas, G., & Moran, E. C. 2001, ApJ, in press [astro-ph/0109246]
Fabbiano, G., Kim, D.-W., & Trinchieri, G. 1992, ApJS, 80, 531
Fabbiano, G. 1996, The Physics of Liners, ASP Conf. Ser., ed. M. Eracleous, A. Koratkar, C. Leitherer, & L. Ho (Baltimore: STScI), 56
Fabbiano, G., & Juda, J. Z. 1997, ApJ, 476, 666 (FJ)
Fabbiano, G., Zezas, A., & Murray, S. S. 2001, ApJ, 554, 1035
Ferrarese, L., & Merritt, D. 2000, ApJ, 539, L9
Fiore, F., Guainazzi, M., & Grandi, P. 1999, Handbook for NFI spectral analysis
http://www.tesre.bo.cnr.it/Sax/software/
Fiore, F., Pellegrini, S., Matt, G., et al. 2001, ApJ, 556, 150
Frontera, F., Costa, E., Dal Fiume, D., et al. 1997, A&AS, 122, 357
Garcia, M., Murray, S. S., Primini, F. A., et al. 2000, ApJ, 537, L23
Gerin, M. R., Casoli, F., & Combes, F. 1991, A&A, 251, 32
Guainazzi, M., & Matteuzzi, A. 1997
http://www.sdc.asi.it/pub/sax/doc/reports/sdc−tr014.ps.gz
Haiman, Z., & Menou, K. 2000, ApJ, 531, 42
Heckman, T. M. 1980, A&A, 88, 365
Heckman, T. M. 2000, Phil. Trans. Royal Soc., Ser. A, 358(1772), 2077
Ho, L. C., Filippenko, A. V., Sargent, W. L. W., & Peng, C. Y. 1997, ApJS, 112, 391
Ho, L. C. 1999, ApJ, 516, 672
Ho, L. C., Feigelson, E. D., Townsley, L. K., et al. 2001, ApJ, 549, L51
Irwin, J. A., Sarazin, C. L., & Bregman, J. N. 2001, submitted to ApJ [astro-ph/0107493]
King, A. R., Davies, M. B., Ward, M. J., Fabbiano, G., & Elvis, M. 2001, ApJ, 552, L109
Kormendy, J., Bender, R., Ajhar, E. A., et al. 1996, ApJ, 473, L91
Larkin, J. E., Armus, L., Knop, R. A., Soifer, B. T., & Matthews, K. 1998, ApJS, 114, 59
Loewenstein, M., Mushotzky, R. M., Angelini, L., & Arnaud, K. A. 2001, ApJ, 555, L21
Makishima, K., Kubota, A., Mizuno, T., et al. 2000, ApJ, 535, 632
Maoz, D., Filippenko, A. V., Ho, L. C., et al. 1995, ApJ, 440, 91
McElroy, D. B. 1995, ApJS, 100, 105
Mulder, P. S., & van Driel, W. 1993, A&A, 272, 63
Nandra, K., George, I. M., Mushotzky, R. F., Turner, T. J., & Yakoob, T. 1997, ApJ, 477, 602
Narayan, R., Igumenischev, I. V., & Abramowicz, M. A. 2000, ApJ, 539, 798
Nicholson, K. L., Reichert, G. A., Mason, K. O., et al. 1998, MNRAS, 300, 893
Parmar, A. N., Martin, D. D. E., Bavdaz, M., et al. 1997, A&AS, 122, 309
Pellegrini, S., & Fabbiano, G. 1994, ApJ, 429, 105
Pogge, R. W. 1989, ApJS, 71, 433
Pogge, R. W., Maoz, D., Ho, L. C., & Eracleous, M. 2000, ApJ, 532, 323
Ptak, A., Serlemitsos, P., Yakoob, T., & Mushotzky, R. F. 1999, ApJS, 120, 179
Quataert, E., Di Matteo, T., & Narayan, R. 1999, ApJ, 525, L89
Richstone, D., Ajhar, E. A., Bender, R., et al. 1998, Nature, 395, A14
Roberts, T. P., Warwick, R. S., & Ohashi, T. 1999, MNRAS, 304, 52 (R99)
Roberts, T. P., & Warwick, R. S. 2000, MNRAS, 315, 98
Schöniger, F., & Sofue, Y. 1997, A&A, 323, 14
Serlemitsos, P., Ptak, A., & Yakoob, T. 1996, The Physics of Liners, ASP Conf. Ser., ed. M. Eracleous, A. Koratkar, C. Leitherer, & L. Ho (Baltimore: STScI), 70
Stark, A. A., Gammie, C. F., Wilson, R. W., et al. 1992, ApJS, 79, 77
Tanaka, Y., & Shibazaki, N. 1996, ARA&A, 34, 607
Terlevich, R., Tenorio-Tagle, G., Franco, J., & Melnick, J. 1992, MNRAS, 255, 713
Thean, A., Pedlar, A., Kukula, M. J., Baum, S. A., & O'Dea, C. P. 2000, MNRAS, 314, 573
Turner, J. L., & Ho, P. T. P. 1994, ApJ, 421, 122
Vignati, P., Molendi, S., Matt, G., et al. 1999, A&A, 349, L57
Ward, M. J., Done, C., Fabian, A. C., Tennant, A. F., & Shafer, R. A. 1988, ApJ, 324, 767
Weisskopf, M. C., O'dell, S. L., & van Speybroeck, L. P. 1996, SPIE, 2805, 2
Wong, T., & Blitz, L. 2000, ApJ, 540, 771
Zezas, A., et al. 2001, in preparation